Analyst

Accepted Manuscript

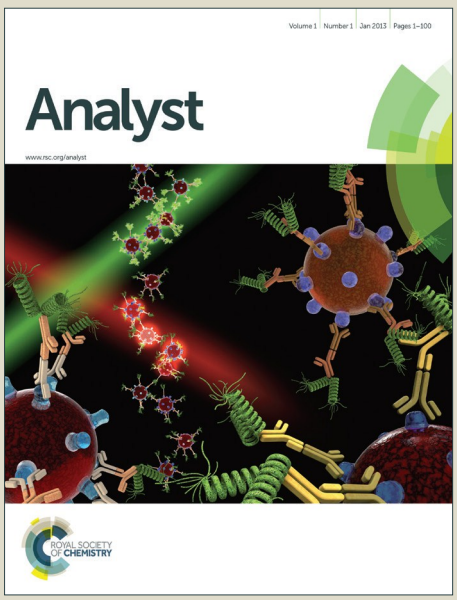

ROYAL SOCIETY OF CHEMISTRY

www.rsc.org/analyst

Journal Name

RSCPublishing

ARTICLE

Sensitive Colorimetric Detection of Protein by Gold Nanoparticles and Rolling Circle Amplification

Cite this: DOI: 10.1039/x0xx00000x

Chaohui Chen, Ming Luo, Tai Ye, Ningxing Li, Xinghu Ji and Zhike He*

Received 00th January 2014,
Accepted 00th January 2014

DOI: 10.1039/x0xx00000x

www.rsc.org/

An ultrasensitive method for the detection of protein is critically important in fundamental research and practical applications due to the low abundance of disease markers in body fluids or tissues. To detect the race levels of disease markers with high sensitivity and specificity, a sensitive colorimetric biosensor for the assay of protein was developed by using of gold nanoparticles (AuNPs) and rolling circle amplification (RCA). After the biotinylated primer/circular template bound to the streptavidin conjugated sandwich ELISA immunocomplex, the biotinylated primer was extended isothermally to generate single-stranded DNA (ssDNA). Sequentially, the padlock DNA was added and hybridized with the products of RCA. Then, the aggregation of the added AuNPs in the supernatant containing surplus padlock DNA and a certain concentration of salt could be observed. The established sensor allowed specific detection of α-fetoprotein (AFP) with a detection limit of 33.45 pg/mL. It was also demonstrated that this method could distinguish 500 pg/mL AFP with the naked eyes. In addition, this biosensor could be applied to complex sample analysis and could be further used as a universal method for any protein or virus determination by changing the corresponding antibodies.

1. Introduction

Highly sensitive detection of trace levels of disease markers is increasingly important in clinical diagnosis, pathology and genetics.[1,2] Polymerase chain reaction (PCR) is the most conventional and frequently-used signal application for ultrasensitive assays. Nevertheless, it is hard to adapt PCR for the measurement of protein because of the intrinsic properties of PCR, such as thermal cycling protocol, time-consuming and requiring expensive instruments.[3] In order to replace the PCR without reducing the sensitive detection ability, rolling circle amplification (RCA) has been developed. RCA is an isothermal enzymatic process where a short primer (DNA or RNA) is amplified to form a long single stranded DNA (ssDNA) or RNA in the presence of a circular template and special polymerases.[4-8] The products of RCA contain tens to hundreds of tandem repeats, which are complementary to the circular template. Besides, RCA can be conducted at a gentle temperature (room temperature to 37 ºC) in solution, on a solid support or even in a complex biological environment. The simplicity and versatility of this amplification technique makes RCA be explored extensively to the detection of DNA[9-11] and proteins.[12-15]

Visual detection, in which the presence of the target can be directly observed by the naked eye, has gained great attention due to the visibility of the target without using any expensive and complicated instruments for this type of assay.[16-20] In the systems of colorimetric detection, gold nanoparticles (AuNPs) have been receiving increasing interest due to the low cost, simplicity, optical and practicality. For colorimetric detection of biomolecules, the gold nanoparticle applications generally rely on the covalently modified nanoparticles and unmodified nanoparticles. For the covalently modified nanoparticles, many researchers have used the gold nanoparticles and DNA conjugates for the detection of DNA and proteins.[21-23] For the unmodified nanoparticles, the detection was based on the discriminated effects of different ssDNA and double stranded (dsDNA) on the aggregations of AuNPs. Since ssDNA can easily bind to citrate-capped AuNPs through the exposed DNA bases-gold interactions and the adsorption of ssDNA can protect the AuNPs against aggregation at high salt concentrations.[24-26] In contrast, repulsion between the negative phosphate backbone of dsDNA and the adsorbed citrate ions makes the dsDNA hard adsorb. Till now, many kinds of AuNPs-based colorimetric assays for protein detection have been reported.[27-31] However, most of these biosensors suffer from the complexity of the experimental system and have difficulty in the detection of complex samples and in practical applications.

Herein, we reported a sensitive colorimetric detection of protein by combing the advantages of RCA and visual detection. In the presence of the target, the biotinylated DNA template could bind to the immunocomplex via biotin-streptavidin interaction and initiate the RCA reaction. Sequentially, the padlock DNA was added and hybridized with the products of RCA. After incubation, the supernatant containing surplus padlock DNA was removed into tubes. Then, AuNPs were added in the supernatant and aggregation of AuNPs was observed at a certain concentration of salt. Without the target, the biotinylated DNA template was washed away and the

reaction of RCA couldn't occur. Thus, the sufficient ssDNA can protect the AuNPs against aggregation. More importantly, this detection strategy cannot only determine the protein by UV-vis absorption intensity but also be realized by photo visualization.

2. Experimental

2.1 Chemicals and reagents

Human α-fetoprotein (AFP) and two monoclonal anti-human AFP antibodies (one antibody is biotinylated) for a sandwich immunoassay and carcinoembryonic antigen (CEA) were ordered from Linc-Bio Science Co., Ltd. (Shanghai, China). T4 DNA ligase and deoxynucleotide solution mixture (dNTP) were purchased from TaKaRa Biotechnology, Co. Ltd. (Dalian, China). The phi29 DNA polymerase was obtained from New England Biolabs, Inc. (Ipswich, MA, USA). Streptavidin (SA) was obtained from Amresco (Solon, OH, USA). Bovine serum albumin (BSA) was purchased from Roche (L.A, CA, USA). Hydrogen tetrachloroaurate (III) trihydrate ($HAuCl_4•3H_2O$) and trisodium citrate were purchased from Sigma-Aldrich (St. Louis, MO, USA). Maxisorp 96 well ELISA microplates were from Thermo Fisher Scientific (Waltham, MA, USA). Human serum sample was supplied by the Zhongnan Hospital of Wuhan University (Wuhan, China). The other chemicals not mentioned here were of analytical-reagent grade or better. DNA oligonucleotides were synthesized and purified by Sangon Biotechnology Co., Ltd (Shanghai, China). The sequences of the oligonucleotides were as follows:

5'-biotin-AAAAAAAAAAAAAAACACAGCTGAGGATAG GACAT-3'

5'-phosphate-CTCAGCTGTGTAACAACATGAAGATTGTA GGTCAGAACTCACCTGTTAGAAACTGTGAAGATCGCT TATTATGTCCTATC-3'

The DNA solution were prepared in 10 mM Tris-HCl buffer (1 mM EDTA, pH 8.00). The phosphate buffer solution (PBS) consisted of 10 mM phosphate buffered saline and 150 M NaCl (pH 7.45). Blocking buffer solution consisted of a PBS solution with added 10% (w/v) bovine serum albumin (pH 7.45). The washing buffer consisted of a PBS solution spiked with 0.1% (v/v) Tween 20 (pH 7.45). DNA hybridization was in the 5 mM Tris-HCl buffer (40 mM NaCl, pH = 8.00).

2.2. Instrumentation

UV-vis measurements were performed with a UV-2250 spectrophotometer (Japan). Gel image was obtained by Molecular Imager Gel Doc XR (USA). Ultrapure water was produced by a Millipore-Q Academic purification set (USA). The pH of solutions was measured by a pB-10 potentiometer (Sartorius).

2.3 Synthesis of AuNPs

The synthesis of AuNPs was performed according previous reports.[32] All glassware used in the synthesis was thoroughly cleaned in aqua regia (HCl/HNO_3, 3:1, v/v), and rinsed in distilled H_2O. A 1 mM $HAuCl_4•3H_2O$ solution (100 mL) was brought to a rolling boil with vigorous stirring. With the rapid addition of 10 mL trisodium citrate (38.8 mM), the solution was in a color change from pale yellow to burgundy. Boiling was maintained for 10 min. After that, the heating mantle was removed, but stirring was continued for about 15 min. Finally, the solution was cooled to room temperature and filtered through a 0.22 μm membrane filter. The average particle size of the AuNPs was about 13 nm from the transmission electron microscopy (TEM) (Figure S1A). An absorption maximum at 520 nm was recorded by using UV-vis spectroscopy (Figure S1B).

2.4 Rolling circle amplification reaction (RCA)

Before amplification reaction, 50 nM biotinylated primer and 50 nM padlock DNA were incubated and hybridized in T4 ligase buffer (30 mM Tris-HCl, 10 mM $MgCl_2$, 1 mM ATP, pH 7.80), followed by the circularization in the presence of 0.4 U/μL ligase at 37 °C for 2 h. After circularization, T4 ligase was inactivated by heating the reaction mixture at 65 °C for 15 min. The resulting circular DNA template could be directly used or stored at 4 °C for further use.

The RCA reaction was performed in the well of microplates. A 50 μL of reaction mixture contained 5 nM circular DNA template, 0.2 mM dNTP, 0.2 mg/mL BSA and 5 U phi29 DNA polymerase was added into the well and the reaction mixture was incubated in polymerase buffer (50 mM Tris-HCl, 10 mM $MgCl_2$, 10 mM $(NH_4)_2SO_4$, pH 7.50) at 37 °C for 4 h.

2.5 Procedure for the detection of AFP

Firstly, a 50 μL of capture antibody (0.02 mg/mL) was immobilized in 96 well microplates overni ght at 4 °C. After decantation of excess antibody, the microplate was blocked by incubating 300 μL of blocking buffer (10% BSA in PBS) for 1 h to prevent nonspecific adsorption. Secondly, the different concentrations of α-fetoprotein (AFP) antigen were added in the plates and incubated for 30 min after rinsing each well three times with PBST buffer. Thirdly, 50 μL of biotinylated antibody (0.02 mg/mL) was bound to antigen for 30 min, followed by incubation of SA (50 μL, 0.02 mg/mL) for 20 min. Subsequently, the amplification of RCA was performed in 96 well microplates. After washing three times, the padlock DNA (23.8 nM) in 5 mM Tris-HCl buffer (40 mM NaCl, pH = 8.00) was added into the well and incubated for 30 min. Finally, the supernatant solution containing surplus padlock DNA was removed into tube and 70 μL of unmodified AuNPs solution was added into it. Ten min later, the UV-vis absorption measurement was performed and the ratio of extinction peak at 658 and 520 nm (A658/A520) was used to analyze the experiment data. The ratio was also associated with the color of the solution, with a high ratio corresponding to a purple solution and a low ratio, to a red one. The procedure of control experiments was similar with the detection of target (Figure S2).

2.6 Selectivity of this method

A 50 μL of the target AFP (1 ng/mL) and the same amount of other proteins were used to test the selectivity of this method according to the procedure of detection of the target protein mentioned above, and the absorption value of each protein was individually measured.

2.7 Gel electrophoresis

After the RCA reaction, the padlock DNA (20 μL, 1 μM) was added and incubated for 30 min, then 10 μL of reaction products was stained with 1× SYBR Green I for 10 min. The products were loaded on 3% agarose gel and electrophoresed in 1×Tris-acetate-EDTA (TAE) buffer (40 mM Tris-AcOH, 2.0 mM Na_2EDTA, pH 8.50) at 100 V for 40 min. The gel was scanned using the Molecular Imager Gel Doc XR.

3. Results and discussions

3.1 Principle of the colorimetric biosensor for protein.

As depicted in Fig. 1, α-fetoprotein (AFP) is selected as the model of protein detection. The SA combined sandwich ELISA immunocomplex binds to the biotinylated primer/circular template when the target AFP is present. In the presence of phi29 DNA polymerase, the biotinylated primer is extended isothermally to generate multimeric ssDNA, which can hybridize with the padlock DNA. Then, the padlock DNA was added and the hybridization was performed. After incubation, the added AuNPs will aggregate in the supernatant containing padlock DNA and a certain concentration of salt, thus a red-to-purple color change of the solution can be obtained. However, without the target AFP, the amplification of RCA can't initiate. All of the added padlock DNA was in supernatant, therefore, AuNPs can be protected from aggregating by the ssDNA. The color change can be detected with the naked eyes and quantified with the UV-vis absorption intensities.

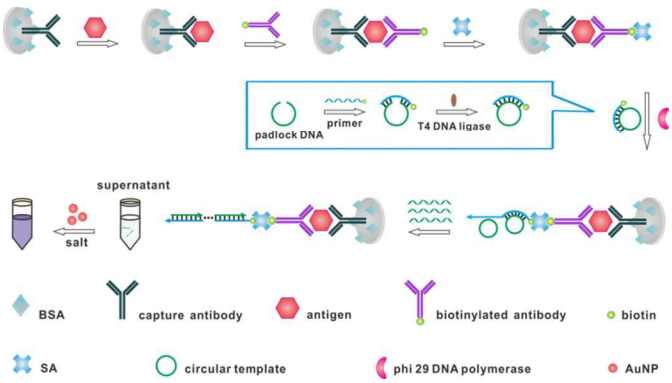

Fig. 1 Schematic illustration of the sensitive colorimetric detection of protein by using of gold nanoparticles and rolling circle amplification.

3.2 The stability of AuNPs by ssDNA

First of all, it was essential to explore the stability of AuNPs under different concentrations of single-stranded padlock DNA. As shown in Fig. 2A, an obvious red-to-purple color change of the AuNPs solution was obtained as the concentration of padlock DNA decreased, and the AuNPs kept red when the concentration of padlock was in the range from 23.8 nM to 167 nM. Meanwhile, in UV-vis spectra (Fig. 2B), the absorption intensities at 520 nm decreased companied with a blue shift with decreased concentration of padlock DNA until 23.8 nM, which was consistent with the colorimetric results. Thus, 23.8 nM padlock DNA was selected for this study. What's more, the effect of salt concentration on the single-stranded padlock DNA coated AuNPs was also studied. As Figure S3 showed, a red-to-purple color change of the AuNPs solution was observed with the increasing concentration of salt in the range from 40 mM to 120 mM and the AuNPs solution kept red when the concentration of salt was below 40 mM. The UV-vis absorption was consistent with the colorimetric results. Thus, 40 mM NaCl was used in this work.

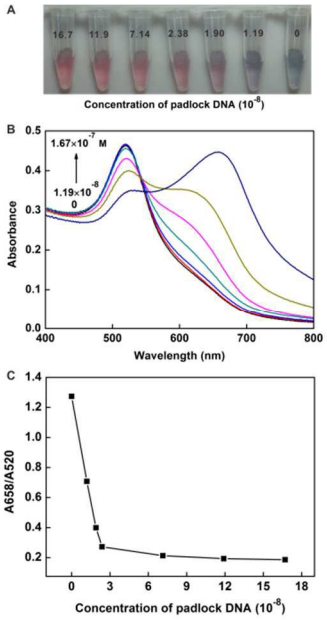

Fig. 2 Color responses of AuNPs in the presence of different concentrations of padlock DNA (ssDNA). From left to right are 1.67×10^{-7}, 1.19×10^{-7}, 7.14×10^{-8}, 2.38×10^{-8}, 1.90×10^{-8}, 1.19×10^{-8}, 0 M. (B) Absorption spectra of the AuNPs in response to various concentrations of padlock DNA (ssDNA). (C) Absorption ratio (A658/A520) was plotted as a function of padlock DNA concentration for the colorimetric assay.

3.3 Verification of the signal amplification strategy

To verify the amplification of the RCA reaction, the products of RCA were first confirmed by 3% agarose gel electrophoresis analysis (Fig. 3A), and a bright band was observed in the presence of phi29. Its migrant rate was even much slower than that of the largest fragment of the DNA marker (1500 bp), demonstrating the formation of multimeric DNA products, indicating the strong ability of RCA to amplify nucleic acid sequences. Compared with lane 1, lane 2 displayed no bands in the absence of phi29, indicating that the RCA reaction was not triggered. In addition, these results were also verified by UV-vis spectra. As shown in Fig. 3B, when there was no AFP in the solution, the immunocomplex could not be formed in the microplate so that the biotinylated primer/circular template was washed away by the washing buffer, thus a high signal (curve a) and no apparent color change were observed (inset in Fig. 3B). A similar phenomenon was exhibited in the absence of phi29 (curve b), this was because the RCA could not be triggered without phi29. Then, the added single-stranded padlock DNA could stabilize AuNPs and effectively prevent them from salt-induced aggregation. While in the presence of target AFP and phi29, the RCA was initiated and part of the added padlock DNA could hybridize with the long ssDNA that formed by the RCA amplification, making a weak absorption spectrum (curve c) and a red-to-purple color change could be observed (inset in Fig. 3B). In addtion, the products of RCA on immobilized template were also confirmed by gel electrophoresis (Figure S4). The results indicated that the efficiency of RCA on immobilized template was lower than homogeneous RCA. However, it still contained tens to hundreds of tandem repeats. All of these results demonstrated that this proposed colorimetric method could be used successfully for the detection of AFP.

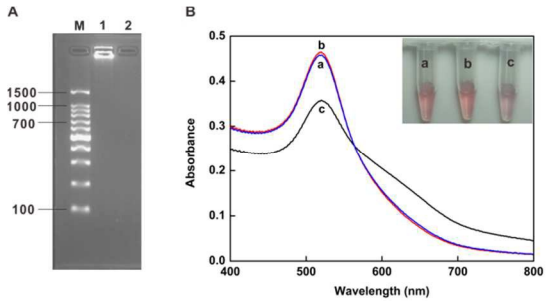

Fig. 3 (A) The gel electrophoresis images of rolling circle amplification products: lane 1, in the presence of phi29 DNA polymerase; lane 2, in the absence of phi29 DNA polymerase; lane M, the DNA ladder marker. (B) UV-vis absorption spectra of the colorimetric detection system under different conditions: (a) in the absence of AFP; (b) in the absence of phi29 DNA polymerase; (c) in the presence of AFP and phi29 DNA polymerase. The inset photograph shows the corresponding color changes.

3.4. Optimization of detection conditions

The parameters affecting RCA process and the UV-vis signal were examined. The effect of the amount of phi29 DNA polymerase on the UV-vis signal was investigated and the result was shown in Figure S5. It was clear that ΔA increased with the increasing amount of polymerase between 1 U and 5 U and reached a plateau after the amount of polymerase was beyond 5 U. Therefore, 5 U phi29 DNA polymerase was used for this research. The reaction time of RCA was studied from 0 to 5 h (Figure S6). ΔA trended to level off at 4 h, indicating the inactivation of the phi29 DNA polymerase, thus, 4 h was selected as the optimal time.

3.5. Sensitivity for the target protein detection

The sensitivity of this proposed method was investigated under the optimal conditions. The color of the AuNPs was gradually changed from red to purple (Fig. 4A) with the increasing concentration of target protein in the range from 50 to 1000 pg/mL. We then studied this system by using UV-vis spectroscopy. As indicated by Fig. 4B, the absorption intensities at 520 nm decreased with an obvious blue shift when the concentration of AFP increased. Accordingly, the absorption peak ratio at 658 and 520 nm was used to determine the protein concentration. The plot of the absorption ratio versus the concentration of AFP was shown in Fig. 4C. A good linear relationship was obtained. The regression equation was $y = 1.9129 \times 10^{-4} x + 0.1410$, where y and x represented the A658/A520 ratio and the target concentration, respectively. A detection limit of 33.45 pg/mL ($\sigma = 3$) was achieved and we could distinguish 500 pg/mL target by the naked eye, which is more sensitive than some other AuNPs-based biosensing.[33,34]

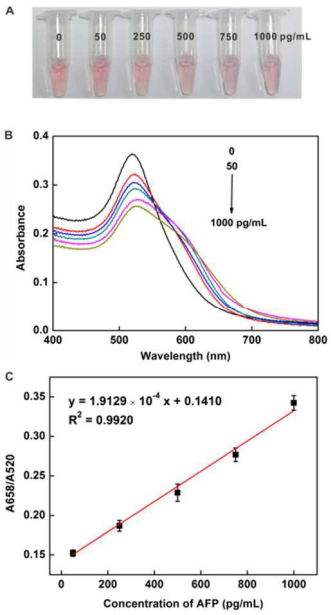

Fig. 4 (A) Color responses of AuNPs in the presence of target AFP with increasing concentrations of 50, 250, 500, 750, 1000 pg/mL from left to right. (B) Absorption spectra of the AuNPs in response to various concentrations of target AFP. (C) Calibration curve of absorption ratio of A658/A520 as a function of the concentration of AFP.

3.6. Selectivity of the target protein detection

As a test of the sensor's specificity, we challenged it with streptavidin (SA), bovine serum albumin (BSA), thrombin and carcinoembryonic antigen (CEA). As the results in Fig. 5 indicated, no aggregations of AuNPs were occurred with the addition of these proteins. In contrast, the color of the AuNPs was changed from red to purple in the presence of target AFP, indicating the high specificity of this method. In addition, the absorption ratio was in consistent with the colorimetric results. The absorption ratio was lower under conditions without the target protein, whereas a higher absorption ratio was observed in the presence of target protein. The high specificity might be attributed to the good specific binding between antibody and antigen.

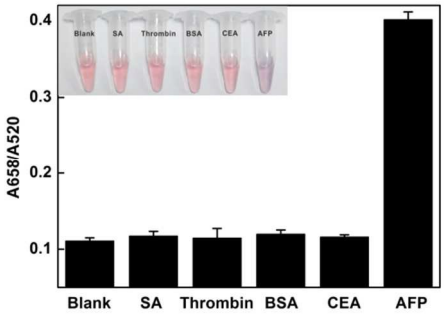

Fig. 5 The absorption ratio of the sensing system in the presence of various proteins. From left to right are blank, SA, Thrombin, BSA, CEA and AFP. The inset shows the corresponding color changes.

3.7 Application to Complex Sample Analysis

A recovery test of AFP in human serum was performed to demonstrate the potential clinical applicability. Human serum samples were 10-fold diluted and spiked with different concentrations of AFP. The analytical results were in table S1 and the quantitative recovery ranged from 94.7% to 103.8%, which was satisfactory for quantitative assays performed in biological samples.

Conclusions

In summary, we have developed a simple, sensitive and highly selective colorimetric detection sensing for protein detection. This biosensor takes advantage of the signal amplification of RCA and visual detection of AuNPs. It has presented high sensitivity for the detection of AFP. The detection limit is calculated to be 33.45 pg/mL by the UV-vis instrument. In addition, this detection model cannot only determine the protein by absorption intensity but also be realized by photo visualization. Furthermore, the method presented here holds promising potential for the detection of any protein or virus by changing the corresponding antibodies.

Acknowledgements

This work was supported by the National Key Scientific Program-Nanoscience and Nanotechnology (2011CB933600), the National Science Foundation of China (21275109, 21205089 and 21475101) and Suzhou Nanotechnology Special Project (ZXG2013028).

Notes and references

Key Laboratory of Analytical Chemistry for Biology and Medicine (Ministry of Education), College of Chemistry and Molecular Sciences, Wuhan University, Wuhan 430072, P. R. China. E-mail: zhkhe@whu.edu.cn; Fax: +86-27-6875-4067; Tel: +86-27-6875-6557

† Electronic Supplementary Information (ESI) available: supplementary figures (Figure S1 ~ Figure S3) and table (table S1). See DOI: 10.1039/b000000x/

1 L. Hood and D. Galas, Nature, 2003, **421**, 444-448.
2 J. Rees; *Science,* 2002, **296**, 698-700.
3 Q. P. Wang, H. Y. Zheng, X. Y. Gao, Z. Y. Lin and G. N. Chen, *Chem. Commun.*, 2013, **49**, 11418-11420.
4 M. Salas, *J. Biol. Chem.*, 2012, **287**, 44568-44579.
5 W. A. Zhao, M. M. Ali, M. A. Brook and Y. F. Li, *Angew. Chem., Int. Ed.*, 2008, **47**, 6330-6337.
6 J. B. Lee, J. Hong, D. K. Bonner, Z. Poon and P. T. Hammond, *Nat. Mater.*, 2012, **11**, 316-322.
7 Z. Deng, Y. Tian, S. H. Lee, A. E. Ribbe, C. Mao, *Angew. Chem.,* 2005, **117**, 3648-3651.
8 W. Zhao, Y. Gao, S. A. Kandadai, M. A. Brook, Y. Li, *Angew. Chem.,* 2006, **118**, 2469-2473.
9 W. Xu, X. J. Xie, D. W. Li, Z. Q. Yang, T. H. Li and X. G. Liu, *Small*, 2012, **8**, 1846-1850.
10 C. Larsson, J. Koch, A. Nygren, G. Janssen, A. K. Raap, U. Landegren, M. Nilsson, *Nat. Methods*, 2004, **1**, 227-232.
11 E. Schopf and Y. Chen, *Anal. Biochem.*, 2010, **397**, 115-117.
12 T. Konry, I. Smolina, J. M. Yarmush, D. Irimia andM. L. Yarmush, *Small*, 2011, **7**, 395-400.
13 L. H. Tang, Y. Liu, M. M. Ali, D. K. Kang, W. A. Zhao and J. H. Li, *Anal. Chem.,* 2012, **84**, 4711-4717.
14 L. Zhou, L. J. Ou, X. Chu, G. L. Shen and R. Q. Yu, *Anal. Chem.*, 2007, **79**, 7492-7500.
15 T. Konry, R. B. Hayman and D. R. Walt, *Anal. Chem.*, 2009, **81**, 5777-5782.
16 S. He, D. Li, C. Zhu, S. Song, L. Wang, Y. Long and C. Fan, *Chem. Commun.*, 2008, **13**, 4885-4887.
17 G. J. Guan, S. Y. Zhang, Y. Q. Cai, S. H. Liu, M. S. Bharathi, M. Low, Y. Yu, J. P. Xie, Y. G. Zheng, Y. W. Zhang, M. Y. Han, *Chem. Commun.,* 2014, **50**, 5703-5705.
18 J. Zhang, C. Yang, X. L. Wang and X. R. Yang, *Analyst*, 2012, **137**, 3286-3292.
19 J. S. Li, J. H. Jiang, X. M. Xu, X. Chu, C. Jiang, G. L. Shen and R. Q. Yu, *Analyst*, 2008, **133**, 939-945.
20 S. Cai, L. Xin, C. Lau and J. Z. Lu, *Analyst*, 2010, **135**, 615-620.
21 C. A. Mirkin, R. L. Letsinger, R. C. Mucic and J. J. Storhoff, *Nature*, 1996, **382**, 607-609.
22 N. L. Rosi and C. A. Mirkin, *Chem. Rev.*, 2005, **105**, 1547-1562.
23 Y. Cao, R. C. Jin, C. A. Mirkin, *Science*, 2002, **297**, 1536-1540.
24 H. X. Li and L. J. Rothberg, *J. Am. Chem. Soc.*, 2004, **126**, 10958-10961.
25 A. P. Xin, Q. P. Dong, C. Xiong and L. S. Ling, *Chem. Commun.*, 2009, **13**, 1658-1660.
26 Y. S. Xing, P. Wang, Y. C. Zang, Y. Q. Ge, Q. H. Jin, J. L. Zhao, X. Xu, G. Q. Zhao and H. J. Mao, *Analyst*, 2013, **138**, 3457-3462.
27 F. Xia, X. L. Zuo, R. Q. Yang, Y. Xiao, D. Kang, A. Vallée-Bélisle, X. Gong, J. D. Yuen, B. Hsu, A. J. Heeger and K. W. Plaxco, *PNAS*, 2010, **24**, 10837-10841.
28 L. J. Ou, P. Y. Jin, X. Chu, J. H. Jiang and R. Q. Yu, *Anal. Chem.*, 2010, **82**, 6015-6024.
29 Y. X. Lu, Y. Y. Liu, S. G. Zhang, S. Wang, S. C. Zhang and X. R. Zhang, *Anal. Chem.*, 2013, **85**, 6571-6574.
30 Y. J. Niu, P. Wang, Y. J. Zhao and A. P. Fan, *Analyst*, 2013, **138**, 1475-1482.
31 W. Li, J. Li, W. B. Qiang, J. J. Xu and D. K. Xu, *Analyst*, 2013, **138**, 760-766.
32 K. Grabar, R. Freeman, M. Hommer and M. Natan, *Anal. Chem.*, 1995, **67**, 735-743.
33 H. Xu, X. Mao, Q. X. Zeng, S. F. Wang, A. N. Kawde and G. D. Liu, *Anal. Chem.*, 2009, **81**, 669-675.
34 N. Thanh and Z. Rosenzweig, *Anal. Chem.*, 2002, **74**, 1624-1628.